Geologica Acta, Vol.16, Nº 3, September 2018, 257-264, I-III
DOI: 10.1344/GeologicaActa2018.16.3.2

geologica acta

Chemical and stable isotope composition ($^{18}O/^{16}O$, $^{2}H/^{1}H$) of formation waters from the Carabobo Oilfield, Venezuela

T. BOSCHETTI[1] B. ANGULO[2] F. QUINTERO[2] J. VOLCÁN[3] A. CASALINS[4]

[1]Department of Chemistry, Life Sciences and Environmental Sustainability, University of Parma
Parco Area delle Scienze, 43124, Parma, Italy. Boschetti E-mail: tiziano.boschetti@unipr.it

[2]Departamento de Investigación Estratégica en Exploración. Instituto Tecnológico Venezolano del Petróleo (INTEVEP), Petróleos de Venezuela S.A. (PDVSA)
Apartado 76343, Caracas 1070-A, Los Teques, Venezuela

[3]Instituto de Ciencias de la Tierra. Universidad Central de Venezuela
Apartado 3895, Caracas 1010-A, Venezuela

[4]Estudios Integrados, Petrolera Sinovensa
Torre BVC, Barcelona 6001, Venezuela

ABSTRACT

In this short note, we present the first data on stable isotope composition of the oilfield waters from Carabobo area of the Faja Petrolífera del Orinoco "Hugo Chávez" (Orinoco Oil Belt). From a chemical point of view, the formation waters show a main Na-Cl level (TDS up to 30g/l) with a dilution trend toward Na-HCO_3 composition (down to 1g/l). Until now, such a clear net chemical compositional trend was ascribed to a meteoric dilution (fresh/brackish bicarbonate) of the seawater endmember (the saltiest chloride). The isotope results of this study reveal that the seawater mother water was modified during a high-temperature thrusting event (120–125°C), forming ^{18}O-enriched diagenetic water (up to +4‰), which was diluted in recent times by glacial meltwater and present-day meteoric water. The hypothetical presence of flood by a meteoric paleo-water also offers new hints to explain the low API gravity (<10°API biodegraded, extra heavy oil) and composition of the local crude.

KEYWORDS | **Orinoco Oil Belt. Carabobo area. Formation water. Chemical and isotope composition.**

INTRODUCTION

The Faja Petrolífera del Orinoco "Hugo Chávez" (FPOHCh; also known in the literature as "Orinoco Oil Belt" or "Orinoco Heavy-Oil Belt") encompasses a territory of approximately 55,000km^2 of the East Venezuela Basin, located in the southern strip of the eastern Orinoco River Basin in Venezuela. With 1.36 trillion barrels of oil-in-place, it is the world's largest onshore oil reserve (Fiorillo, 1987; Schenk *et al*., 2009; Petróleos de Venezuela S.A.-Corporación Venezolana del Petróleo, 2013). The deposition of the oil source rocks occurred on the northern passive continental margin (Cretaceous to Paleogene). Since the Oligocene-Miocene, a southward migration of the oil occurred in the foreland basin during the fold-thrust belting, which involved a North-South crustal shortening of 40% or more, forming a flexural forebulge against the Guyana shield (Talukdar *et al*., 1988). The main southward migration of meteoric and connate/formation waters has been modeled and theorized in several studies (Gallango

and Parnaud, 1995; Parnaud *et al*., 1995; Schneider, 2003; Schneider, 2005). However, an isotopic analysis of the local oilfield waters was still lacking. In this study, the origin of the Carabobo's formation waters is inferred from the chemical and isotope water composition.

GEOLOGIC OUTLINES

The extraction area of the FPOHCh is subdivided from West to East in four administrative areas (Fig. I in the Electronic Appendix): Boyacá and Junín, mainly located in the western Guárico sub-basin; and Ayacucho and Carabobo, mainly located in the eastern Maturín sub-basin. The water samples of this study were collected from boreholes within the Monagas state, in the central sector of the Carabobo area, previously known as Cerro Negro (Fiorillo, 1987). In this area, the Las Piedras (Upper Miocene/Pliocene) and Mesa (Pleistocene) sandstone formations are at the upper part of the stratigraphic column (Fig. II in Electronic Appendix). Often undistinguishable, these formations do not contain hydrocarbons but fresh-to-brackish groundwater of the Mesa/Las Piedras regional aquifer (Montero *et al*., 1998; Petroleos de Venezuela S.A., 1999; De Freitas and Coronel, 2012). Beneath, the Freites Formation (Fm.) (Middle Miocene) consists of shale and sandstones. It conformably overlies the Oficina Fm. (Middle-Upper Miocene), which represents the most productive reservoir. It is subdivided in four members (from base to top): Moríchal, Yabo, Jobo, and Pilón. In particular, the sandstones of the Moríchal Member have the best reservoir quality, with 32% porosity and 10Darcy permeability on average (Lugo *et al*., 2001). One interpretation is that these sands deposited in valley fairways, with valley incision controlled by climate and sea-level changes, thus forming a transgressive sequence with fluvial sands at the base and marginal marine sands near the top (Gary *et al*., 2001). In the study area, the Moríchal reservoir sands are 100m-thick on average and unconformable overlie the Precambrian igneous and metamorphic basement. The top of the basement is located at a depth of approximatively 850–900m (Santos and Frontado, 1987; Pérez, 2010; Gil, 2017). Water recharges came from Serranía del Interior (North) and the Guyana Shield (South), but in the Oligocene-Miocene reservoir, a deep groundwater drainage from West to East also occured (Parnaud *et al*., 1995; Bartok, 2003; Martinius *et al*., 2013). The main geologic structure of the Oficina Fm. is represented by a regional monocline, striking East-West and dipping 3ºN (the ramp of the peripheral bulge). Normal faults and fault blocks were caused by lithostatic charges over the crystalline basement. Minor structures consist of sequences of uplifted and depressed blocks in alternating sequences (Santos and Frontado, 1987; González and Meaza, 2014).

METHODS

Water samples from thirteen wells, which draw crude oil from the Oficina (C4–C13) and Freites formations (C1–C3), were collected during 2014–2016 for physicochemical and isotope measurements. These wells were chosen because they were not affected by waterflooding (*i.e*. use of water injection to enhance production) and had a water production higher than 40% (Boschetti *et al*., 2016). All water samples were not in emulsion with the crude and showed spontaneous separation from organic fraction after 24h, except for sample C4. In the latter case, water was extracted after emulsion destabilization and demulsification using the procedure described in Boschetti *et al*. (2016). Then, all water samples were passed through a funnel filled with glass wool to guarantee the elimination of crude residuals. Physicochemical parameters were determined according to Boschetti *et al*. (2016). The oxygen and hydrogen stable isotope ratios of water molecules, $\delta^{18}O(H_2O)$ and $\delta^{2}H(H_2O)$, were analyzed at the Stable Isotope Laboratory of the Instituto Andaluz de Ciencias de la Tierra (Consejo Superior de Investigaciones Científicas-Universidad de Granada, Granada, Spain) by, a high-Temperature Conversion/Elemental Analyzer (TC/EA) coupled online with an Isotope Ratio Mass Spectrometer (IRMS, Delta XP, Thermo-Finnigan, Bremen). Samples for isotopic analysis were passed through activated carbon for organic compounds remotion. After that, an aliquot of 0.7µl was injected into the reactor of the elemental analyzer, a ceramic column containing a glassy carbon tube kept at 1450ºC, to produce H_2 and CO gases (Sharp *et al*., 2001; Rodrigo-Naharro *et al*., 2013). Five different internal laboratory standards ($\delta^{18}O$; $\delta^{2}H$) IACT-2 (+7.28‰; +57.42‰), EEZ3B (+1.05‰; +7.90‰), CAN (-3.70‰; -17.50‰), GR-08 (-8.35‰; -55.00‰) and SN-06 (-10.61‰; -72.77‰), were employed for instrumental calibration. These were previously calibrated against certified international standards from the International Atomic Energy Agency: V-SMOW, GISP and SLAP (NIST codes RM8535, RM8536 and RM8537, respectively). To avoid memory effects, each sample was analyzed ten times, discarding the first five results and doing average on the last five. The calculated precision, after correction of the mass spectrometer daily drift from previously calibrated internal standards systematically interspersed in the analytical batches (Rodrigo-Naharro *et al*., 2013), was better than ±0.2‰ for oxygen and ±1‰ for hydrogen. Local groundwater (Mesa/Las Piedras) and surface water from a river (Río Moríchal) were also analyzed for isotope composition and chloride concentration.

RESULTS AND DISCUSSION

The obtained results are shown in the Electronic Appendix (Table I). An additional chemical dataset of

24 oilfield waters from the Carabobo area, collected and analyzed during 2017 (Table II, Electronic Appendix) was also used to interpret the chemical processes.

Chemical composition

When plotted in the Langelier-Ludwig plot (Boschetti, 2011), formation waters from the FPOHCh had a Na-Cl main composition with brackish to saline Total Dissolved Solids (TDS) up to approximatively 30g/l, and the saltiest waters plot close to the "marine-side" of the diagram (Fig. 1). The Cl/Br ratio <286mg/l (211±38) also testifies a seawater origin, probably modified by the reaction with minerals of the basement and/or by ternary mixing between meteoric water, seawater and a seawater-evaporated brine (Rosenthal, 1997; McCartney and Rein, 2005; Sonney and Vuataz, 2010). Only the sample C1 from the Freites Formation showed a Na-HCO_3 composition (Fig. 1) and was characterized by a lower TDS 1g/l. The chemical trend depicted in the diagram was consistent with the

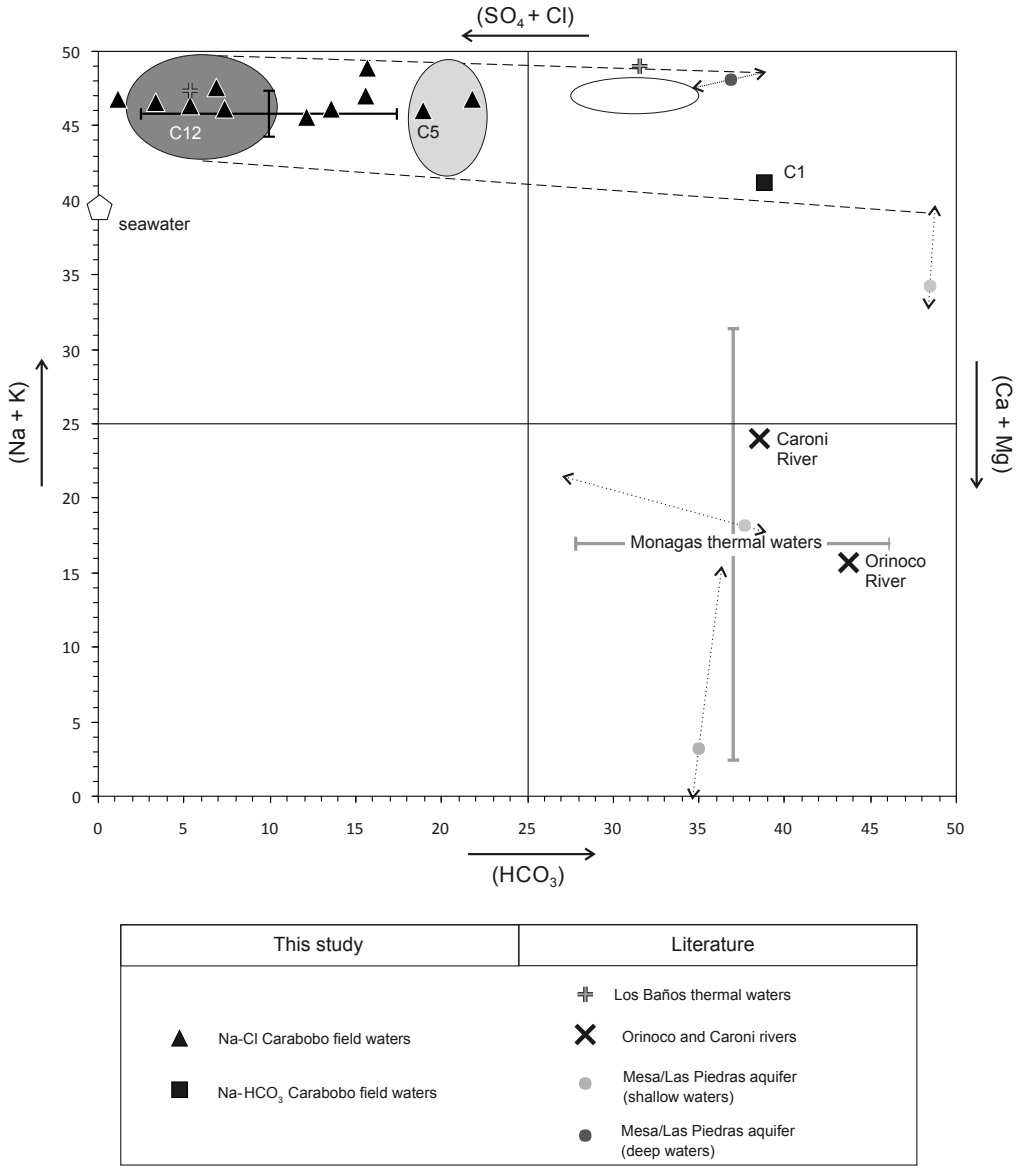

FIGURE 1. Langelier-Ludwig diagram (Boschetti, 2011) of the oilfield waters from Carabobo area (meq/L basis): Na-Cl (triangles: data from Table I, Electronic Appendix; dark error bars: average and standard deviations from Table II , Electronic Appendix. Appendices available at www.geologica-acta.com) and Na-HCO_3 (squares: C1 sample in the Table I, Electronic Appendix). Dashed lines show the compositional variation trend. Following this trend, the three different oilfield waters detected in the Junín area (Marcos *et al.*, 2007) are shown by ellipses for comparison purposes: Na-Cl brine (dark gray); Na-HCO_3 meteoric (white); mixed (light gray). Dots with arrows show the average and variation trend, respectively, of the shallow (light gray dots) and deep (dark gray dots) components of the Mesa/LasPiedras aquifer (De Freitas and Coronel, 2012). The Ca-HCO_3 composition of the Orinoco and Caroni Rivers (X) (Lewis and Weibezhan, 1981; Lewis *et al.*, 1995) and thermal waters in Monagas state (Hernández and Sánchez, 2004) are also shown. An exception from the shallow Ca-HCO_3 composition is represented by Na-HCO_3 to Na-Cl composition of the Los Baños thermal spring (+), which is mixed with oil seeps (Urbani, 1989).

preliminary investigations in the Carabobo area (Pirela *et al.*, 2008), in the Oficina Member formation waters from the Anaco Field (central Anzoátegui state; Funkhouser *et al.*, 1948) and in the Junín area of the FPOHCh (Marcos *et al.*, 2007). In all studies concerning the FPOHCh, three different members were distinguished in the area: Na-Cl brines, Na-Cl intermediate and Na-HCO_3 meteoric. Figure 1 shows that the formation waters that are more affected by the "meteoric Na-HCO_3 member" compositionally correspond to the deepest groundwater of the Mesas-Las Piedra aquifer (De Freitas and Coronel, 2012). As revealed in the Anaco Fields, groundwater flow could also occur deeply in the Oficina Formation, as evidenced by pressure switch (Funkhouser *et al.*, 1948; Tackett, 2008). However, in comparison with the Oficina Formation, our Carabobo's Na-HCO_3 sample C1 is more closely shifted toward the Ca-HCO_3 field, which is the most common composition of the local shallow groundwater (De Freitas and Coronel, 2012). The Orinoco River (Lewis and Weibezhan, 1981; Lewis *et al.*, 1995) and most of the thermal waters of the Monagas state (Hernández and Sánchez, 2004) also showed a Ca-HCO_3 composition, with the exception of the H_2S-bearing spring of Los Baños. In the diagram (Fig. 1), this spring falls within the formation water trend because it has probably been affected by oil seep (Urbani, 1989).

Isotope composition

Most of the sampled waters plot below the Global Meteoric Water Line (Gourcy *et al.*, 2007) (Fig. 2A), clustering between the mean values of the Orinoco River at Ciudad Bolivar (International Atomic Energy Agency/ World Meteorological Organization, 2017a) and the seawater and/or porewaters from the Venezuela Basin (Friedman and Hardcastle, 1973; Lawrence, 1973). The waters of the first cluster, -35‰<$\delta^2H(H_2O)$<-20‰, fall close to the area containing the samples of the Maracaibo Oilfield (Boschetti *et al.*, 2016). However, differently from this latter, the contribution of meteoric water in the Carabobo formation waters is probably more important than an ^{18}O-enriched diagenetic water (Fig. 2A). Indeed, the Na-HCO_3 sample C1 showed the most depleted $\delta^2H(H_2O)$, falling between the Moríchal and Orinoco Rivers (Fig. 2A). In the second seawater-derived samples cluster, -10‰<$\delta^2H(H_2O)$<0‰, the sample C5 showed a prominent O-shift on the right side of the water line up to $\delta^{18}O(H_2O)$=+4‰. This ^{18}O-enrichment, commonly associated with water-rock interaction processes, could be attributed to a diagenetic effect. Accordingly, an estimated $\delta^{18}O$ composition between +2‰ and +6‰ was related to the formation fluids, which precipitate quartz at a temperature of 100–125°C during the southward thrusting event (Schneider, 2005). Indeed, when the Na-Li geothermometer for sedimentary brines (Sanjuan *et al.*, 2014) was applied to the concentrations of the two elements obtained in this study, a mean temperature of 125±5°C was recorded. This temperature is significantly higher than the present-day temperature at the bottom hole (not higher than 60°C, also according to the present-day local geothermal gradients (Fiorillo, 1987; Quigiada, 2006) but is consistent with temperatures achieved during the quartz cementation process during the Miocene thrusting (Roure *et al.*, 2010). Finally, a deuterium-chloride diagram (Fig. 2B) confirmed that local Na-Cl formation waters derive from marine porewaters, which were diluted by two main end-members: diagenetic waters with $\delta^2H(H_2O)$ similar to porewater (sample C5), and inflows from present-day meteoric water (samples C1, C8), *e.g.* Orinoco River with $\delta^2H(H_2O)$=-41‰ (International Atomic Energy Agency/World Meteorological Organization, 2017b). We hypothesize that a third end-member could be meltwater from the last glaciation, with a $\delta^2H(H_2O)$ of approximatively -145‰ (Ramirez *et al.*, 2003), which probably diluted sample C12 as similarly expected in different studied sites (Birkle *et al.*, 2009; Boschetti *et al.*, 2016). As opposed to other oilfield waters from the study area, this latter sample falls very close to the Meteoric Water Line (Fig. 2A) and on the seawater-meltwater binary mixing curve (Fig. 2B), showing a substantially unchanged chloride content similar to the porewaters. Considering the lack of chloride-bearing evaporite minerals in the formations at depth, and according to Warne *et al.*(2002), this glacial melts-seawater mixing probably occurred in the Orinoco area at approximatively 18,000-15,000yrs BP. However, at this stage of the investigation we cannot exclude the possible contribution of meteoric paleo-water of different age. For example, isotope composition of the rainfall during the last 14,000 years was not so different from that of the present-day, -45‰<$\delta^2H(H_2O)$<-28‰ and -8 ‰<$\delta^{18}O(H_2O)$<-4‰ (Van Breukelen *et al.*, 2008), thus representing another potential source of the local formation waters (Fig. 2).

CONCLUSIONS

In this study, a Na-Cl main composition of the Carabobo oilfield waters from the Moríchal Member, with a dilution trend toward Na-HCO_3 due to the influx of diluted and shallow waters, was revealed. These findings agree in part with the results previously obtained by other authors (Pirela *et al.*, 2008). The novelty of our work lies in the discrimination of the isotope signature of these waters. Our results highlight i) the seawater origin of the deep Na-Cl endmember, which resembles the porewaters of the Venezuela Basin; and ii) the presence of three additional, isotopically different waters, which can shift the composition of the mother salty porewater toward a high $\delta^{18}O(H_2O)$ (diagenetic water from quartz cementation) or low $\delta^2H(H_2O)$ (meteoric components from the last glaciation to the present). Such chemical-isotope

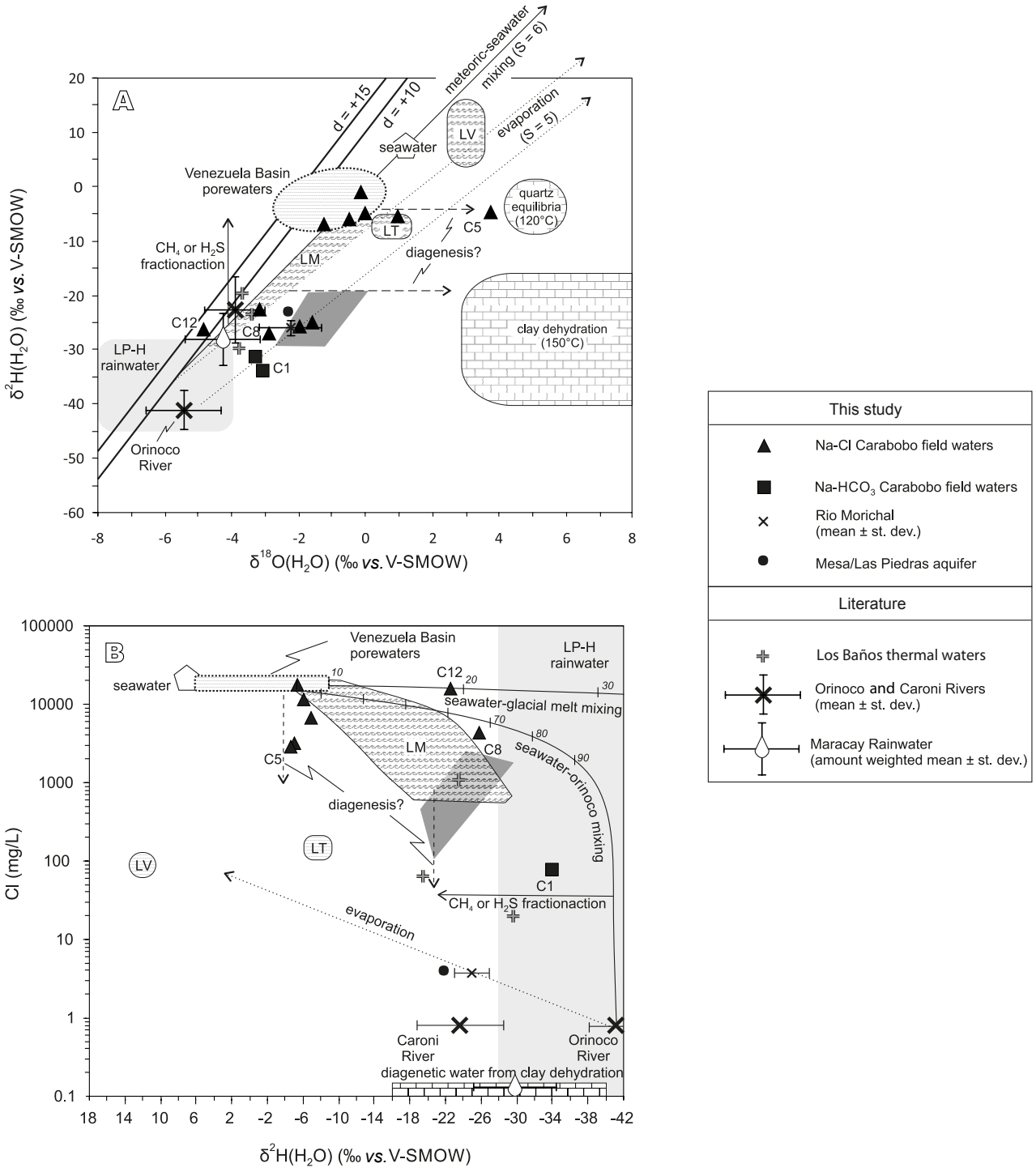

FIGURE 2. A) $\delta^2H(H_2O)$ *vs.* $\delta^{18}O(H_2O)$ and B) chloride (mg/L) *vs.* $\delta^2H(H_2O)$ diagrams, modified from Boschetti *et al.* (2016). Na-Cl (triangles) and Na-HCO_3 (squares) oilfield waters from Carabobo area (this study) and Lake Maracaibo (dark gray field) (Boschetti *et al.*, 2016) are shown. Global (d=+10) and local (d=+15) meteoric water lines are shown in A). The mean composition of Orinoco and Caroni rivers (International Atomic Energy Agency/Water Resources Programme, 2009; International Atomic Energy Agency/World Meteorological Organization, 2017b), Maracay rainwater (International Atomic Energy Agency/World Meteorological Organization, 2017a), Los Baños thermal waters (Urbani, 1989) and Late Pleistocene–Holocene rainfall (LP-H light gray field; Van Breukelen *et al.*, 2008) are plotted in both diagrams. Lake Maracaibo (LM), Lake Valencia (LV) and Lagoon Taguaiguay (LT) are also plotted in both diagrams to represent the fractionation effect due to evaporation (Boschetti *et al.*, 2016). As opposed to Maracaibo oilfield waters, which showed ^{18}O-enrichment due to clay dehydration, the Carabobo waters show an ^{18}O-shift, probably due to quartz equilibrium during the thrusting event in Maturín Sub-basin, starting from Venezuela Basin porewater. In the plot B), the inflows of present-day meteoric water (δ^2H=-43‰, Cl=1mg/l) on C8, C1 samples and a hypothetical last glaciation floodwater (δ^2H=-145‰, Cl=1mg/l) on C12 are also distinguishable. Curves represent binary mixings: numbers in italic are the percentage of the aforementioned diluting waters. See text for details. The fractionation effect due diagenesis (dashed arrow; Boschetti *et al.*, 2016) and to hydrogen-bearing gases (solid arrow; Clark, 2015) are also shown in both diagrams.

differentiation of the waters is the result of a complex history combined with the particular structural settings of the studied area (peripheral bulge, stratigraphic pinch-outs, normal faults). Additional chemical and isotopic analyses (along with ^{14}C data) of waters from the neighbouring boreholes are necessary to better decipher the paleo-recharge and provenance of the meteoric waters (*i.e.* Serranía del Interior, Guyana Shield, Orinoco). However, until now, only generic meteoric water was considered in a hydrodynamic model and biodegradation process during heavy oil formation (Parnaud *et al.*, 1995; Talwani, 2002). The flood of the oil reservoir by a meteoric paleo-water could also help to explain the extreme degradation of the oil in this area (Larter and Head, 2014).

ACKNOWLEDGMENTS

We would like to thank Dr. A. Delgado, Consejo Superior de Investigaciones Científicas (CSIC)-Instituto Andaluz de Ciencias de la Tierra, Granada, Spain, for the isotope analyses. Petróleos de Venezuela S.A. and the oil companies participating in the local joint ventures (Petromonagas, Petrolera Sinovensa, Petroindependencia) are also thanked for allowing us to conduct this research, their support during sampling and permission to publish the data. The comments made by anonymous reviewers were highly appreciated.

REFERENCES

Audemard, F., Azpiritxaga, Y., Baumann, P., Isea, A. Latreille, M., 1985. Marco geológico del terciario en la Faja Petrolífero del Orinoco de Venezuela. Proceedings of the 6th Venezuelan Geological Congress, Caracas, Proceedings, Sociedad Venezolana de Geólogos (SVG) Memoir, 1, 70-108.

Bartok, P., 2003. The peripheral bulge of the Interior Range of the Eastern Venezuela Basin and its impact on oil accumulations. In: Bartolini, C., Buffler, R.T., Blickwede, J. (eds.). The Circum-Gulf of Mexico and the Caribbean: Hydrocarbon habitats, basin formation, and plate tectonics. American Association of Petroleum Geologists (AAPG) Memoir, 79, 925-936.

Birkle, P., Martínez, B.G., Milland, C.P., Eglington, B., 2009. Origin and evolution of formation water at the Jujoe-Tecominoacán oil reservoir, Gulf of Mexico. Part 2: isotopic and field-production evidence for fluid connectivity. Applied Geochemistry, 24, 555-573.

Boschetti, T., 2011. Application of Brine Differentiation and Langelier-Ludwig plots to fresh-to-brine waters from sedimentary basins: diagnostic potentials and limits. Journal of Geochemical Exploration, 108, 126-130.

Boschetti, T., Angulo, B., Cabrera, F., Vásquez, J., Montero, R.L., 2016. Hydrogeochemical characterization of oilfield waters from southeast Maracaibo Basin (Venezuela): Diagenetic effects on chemical and isotopic composition. Marine and Petroleum Geology, 73, 228-248.

Clark, I., 2015. Groundwater Geochemistry and Isotopes. CRC Press - Taylor & Francis Group, Boca Raton, FL, USA, 421pp.

De Freitas, F.J., Coronel, A., 2012. Caracterización hidrogeoquímica de las aguas subterráneas del acuífero Mesa-Las Piedras, Venezuela. Revista Latino-Americana de Hidrogeología, 8(1), 9-19.

Fiorillo, G., 1987. Exploration and evaluation of the Orinoco Oil Belt. In: Meyer, R.F. (ed.). Exploration for heavy crude oil and natural bitumen. American Association of Petroleum Geologists (AAPG), Studies in Geology, 25, 103-121.

Friedman, I., Hardcastle, K., 1973. Interstitial water studies. Leg 15 - Isotopic composition of water, Washington, D.C., USA, 901-903.

Funkhouser, H.J., Sass, L.C.,Hedberg, H.D., 1948. Santa Ana, San Joaquín, Guario, and Santa Rosa oil fields (Anaco fields), Central Anzoátegui, Venezuela. American Association of Petroleum Geologists (AAPG) Bulletin, 32, 1851-1908.

Gallango, O., Parnaud, F., 1995. Two-dimensional computer modeling of oil generation and migration in a transect of the Eastern Venezuela basin. In: Tankard, A.J., Suárez Soruco, R., Welsink, H.J. (eds.). Petroleum Pasins of South America. American Association of Petroleum Geologists (AAPG), Memoir, 62, 727-740.

Gary, R., Rene, S., Milton, V., 2001. Geologic reality altered Cerro Negro development scheme. Oil and Gas Journal, 99(4), 37-43.

Gil, L.A., 2017. Interpretación sísmica 3D Mb Moríchal del bloque petrolera Sinovensa, Faja Petrolífera del Orinoco. Master Thesis, Universidad Simón Bolívar, Venezuela, 126pp.

González, P., Meza, R., 2014. Construction of Training Images Using Seismic Attributes to delineate Braided Channels in Moríchal Member, Oficina Formation, Faja Petrolífera del Orinoco, Venezuela. Proceedings of the Heavy Oil Latin America Conference & Exhibition, Venezuela, HOLA14, 161, 10pp.

Gourcy, L.L., Groening, M., Aggarwal, P.K., 2007. Stable oxygen and hydrogen isotopes in precipitation. In: Aggarwal, P.K., Gat, J.R., Froehlich, K.F.O. (eds.). Isotopes in the Water Cycle: Past, Present and Future of a Developing Science. Springer, Dordrecht, the Netherlands, 39-51.

Hernández, C.D.C., Sánchez, R.S.N., 2004. Distribución, caracterización y marco teórico de las aguas termales en Venezuela. Degree Thesis, Universidad Central de Venezuela, Caracas, 819pp.

International Atomic Energy Agency/World Meteorological Organization, 2017a. Global Network of Isotopes in Precipitations. The GNIP Database. Accessible at: www-naweb.iaea.org/napc/ih/IHS_resources_gnip.html. Accessible at: www.nucleus.iaea.org/wiser/index.aspx. [Last accessed: 12 June 2018]

International Atomic Energy Agency/World Meteorological Organization, 2017b. Global Network of Isotopes in Rivers.

The GNIR Database. Accessible at: www.nucleus.iaea.org/wiser/index.aspx [Last accessed: 12 June 2018]

International Atomic Energy Agency/Water Resources Programme, 2009. Part II: South America, Venezuela. In: Atlas of Isotope Hydrology -the Americas- International Atomic Energy Agency. Water Resources Programme, Austria, 147-155.

Larter, S.R., Head, I.M., 2014. Oil Sands and Heavy Oil: Origin and Exploitation. Elements, 10, 277-284.

Lawrence, J.R., 1973. Interstitial water studies. Leg 15 - Oxygen and carbon isotope variations in water, carbonates and silicates from the Venezuela Basin (Site 149) and the Aves Rise (Site 148), Washington, D.C., USA, 891-899.

Lewis, M.W.J., Weibezhan, F., 1981. The chemistry and phytoplankton of the Orinoco and Caroni Rivers, Venezuela. Archiv für Hydrobiologie, 91(4), 521-528.

Lewis, W.M.J., Hamilton, S.K., Saunders, J.F.I., 1995. Rivers of Northern South America. In: Cushing, C., Cummisn, K. (eds.). Ecosystems of the World: Rivers. Elsevier, Dordrecht, The Netherlands, 219-256.

Lugo, R.G., Eggenschwiler, M., Uebel, T., 2001. How Fluid and Rock Properties Affect Production Rates in a Heavy-Oil Reservoir Cerro Negro, Venezuela, Society of Petroleum Engineers Inc. International Thermal Operations and Heavy Oil Symposium, 12-14 March, Porlamar, Margarita Island (Venezuela), 8pp.

Marcos, J., Pardo, E., Casas, J., Delgado, D., Rondon, M., Exposito, M., Zerpa, L., Ichbia, J., Bellorini, J.P., 2007. Static and Dynamic Models of Formation Water in Sincor Area, Orinoco Belt, Venezuela, Society of Petroleum Engineers Inc., Latin American and Caribbean Petroleum Engineering Conference, SPE 107378. Buenos Aires (Argentina), 11pp.

Martinius, A.W., Hegner, J., Kaas, I., Bejarano, C., Mathieu, X., Mjøs, R., 2012. Sedimentology and depositional model for the Early Miocene Oficina Formation in the Petrocedeño Field (Orinoco heavy-oil belt, Venezuela). Marine and Petroleum Geology, 35(1), 354-380.

Martinius, A.W., Hegner, J., Kaas, I., Mjøs, R., Bejarano, C., Mathieu, X., 2013. Geologic reservoir characterization and evaluation of the Petrocedeno Field, Early Miocene Oficina Formation, Orinoco Heavy Oil Belt, Venezuela. In: Hein, F.J., Leckie, D., Larter, S., Suter, J.R. (eds.). Heavy-oil and oil-sand petroleum systems in Alberta and beyond. American Association of Petroleum Geologists, Studies in Geology, 64, 103-131.

McCartney, R.A., Rein, E., 2005. Formation waters of the Norwegian Continental Shelf, Tekna. 16th International Oil Field Chemistry Symposium, 13-16 March, Geilo (Norway), 6pp.

Montero, R.L., López, C., Yanes, C., Meléndez, W., Vargas, M., 1998. Estudio geoquímico de las aguas subterráneas de Los Llanos Orientales de Venezuela. In: Carillo Castellano, R.J. (eds.). Memorias IV. Congreso Interamericano sobre el medio ambiente. Tomo 1. Equinoccio. Ediciones de la Universidad Simón Bolívar, Caracas, Venezuela, 87-91.

Parnaud, F., Gou, Y., Pascual, J.-C., Truskowski, I., Gallango, O., Passalacqua, H., Roure, F., 1995. Petroleum Geology of the Central Part of the Eastern Venezuelan Basin. In: Tankard, A.J., Suárez Soruco, R., Welsink, H.J. (eds.). Petroleum basins of South America, American Association of Petroleum Geologists, Memoir, 62, 741-756.

Petroleos de Venezuela S.A., 1999. Léxico Estratigráfico de Venezuela; Petroleos de Venezuela S.A. - Intevep. Accessible at: www.lev.desarrollominero.gob.ve/ [Last accessed: 12 June 2018]

Petróleos de Venezuela S.A., Corporación Venezolana del Petróleo (PDVSA-CVP), 2013. Atlas de integración regional de la Faja Petrolífera del Orinoco. Caracas, Proyecto Orinoco Magna Reserva. Editorial Arte, 133pp.

Pérez, L.E.P., 2010. Propuesta de un modelo estratigráfico a nivel de la arena O-12 de la Formación Oficina de los Yacimientos OFIM CN 42 Y OFIM CNX 3, área J-20 pertenecientes al Campo Cerro Negro – Bloque Carabobo – Faja Petrolífera del Orinoco del Distrito Moríchal, Estado Monagas, Venezuela. Master Thesis, Universidad de Oriente, Ciudad Boíivar (Venezuela), 113pp.

Pirela, M., García, J.A., Rondón, J., 2008. Geochemical characterization and origin of Carabobo's area formation water, Orinoco Oil Belt, Venezuela, XV World Water Congress - International Water Resources Association, 25-29 May, Edinburgh, Scotland. Accessible at: www.iwra.org/member/congress/resource/abs276_article.pdf [Last accessed: 12 June 2018]

Quigiada, B.M.J.H., 2006. Modelado numérico termal 1D de la Cuenca Oriental de Venezuela. Master Thesis, Universidad Simón Bolívar, 142pp.

Ramirez, E., Hoffmann, G., Taupin, J.D., Francou, B., Ribstein, P., Caillon, N., Ferron, F.A., Landais, A., Petit, J.R., Pouyaud, B., Schotterer, U., Simoes, J.R. and Stievenard, M., 2003. A new Andean deep ice core from Nevado Illimani (6350 m), Bolivia. Earth and Planetary Science Letters, 212(3-4), 337-350.

Rodrigo-Naharro, J., Delgado, A., Herrero, M.J., Granados, A., Pérez del Villar, L., 2013. Current Travertines Precipitation from CO_2-rich Groundwaters as an Alert of CO_2 Leakages from a Natural CO_2 Storage at Gañuelas-Mazarrón Tertiary Basin (Murcia, Spain). Consejería de Medio Ambiente y Ordenación del Territorio, Madrid, España, 53pp. Accessible at: www.documenta.ciemat.es/handle/123456789/77 [Last accessed: 12 June 2018]

Rosenthal, E., 1997. Thermomineral waters of Ca-chloride composition: review of diagnostics and of brine evolution. Environmental Geology, 32(4), 245-250.

Roure, F., Andriessen, P., Callot, J.P., Faure, J.L., Ferket, H., Gonzales, E., Guilhaumou, N., Lacombe, O., Malandain, J., Sassi, W., Schneider, F., Swennen, R., Vilasi, N., 2010. The use of palaeo-thermo-barometers and coupled thermal, fluid flow and pore-fluid pressure modelling for hydrocarbon and reservoir prediction in fold and thrust belts. In: Goffey, G.P., Craig, J., Needam, T., Scott, R. (eds.). Hydrocarbons in

Contractional Belts. Geological Society of London, Special Publications, 348, London, 87-114.

Sanjuan, B., Millot, R., Asmundsson, R., Brach, M., Giroud, N., 2014. Use of two new Na/Li geothermometric relationships for geothermal fluids in volcanic environments. Chemical Geology, 389, 60-81.

Santos, A., Frontado, L., 1987. Reservoir geology of the Cerro Negro steam injection area, Orinoco Oil Belt, Venezuela. Journal of Petroleum Geology, 10(2), 177-194.

Schenk, C.J., Cook, T.A., Charpentier, R.R., Pollastro, R.M., Klett, T.R., Tennyson, M.E., Kirschbaum, M.A., Brownfield, M.E., Pitman, J.K., 2009. An Estimate of Recoverable Heavy Oil Resources of the Orinoco Oil Belt, Venezuela. World Petroleum Resources Project, Fact Sheet 2009–3028. United States Department of the Interior, United States Geological Survey, pp. 4. Accessible at: www.pubs.usgs.gov/fs/2009/3028/pdf/FS09-3028.pdf [Last accessed: 12 June 2018]

Schneider, F.J.S., 2003. Basin Modeling in Complex Area: Examples from Eastern Venezuelan and Canadian Foothills. Oil and Gas Science and Technology, 58, 313-324.

Schneider, F.J.S., 2005. Understanding the diagenetic evolution of potential reservoirs in fold/thrust belts: an example from eastern Venezuela. In: Doré, A.G.,Vining, B.A. (eds.). Petroleum Geology: North-West Europe and Global Perspectives. Proceedings of the 6th Petroleum Geology Conference. Geological Society of London, London, 1359-1366.

Sharp, Z.D., Atudorei , V., Durakiewicz, T., 2001. A rapid method for determination of hydrogen and oxygen isotope ratios from water and hydrous minerals. Chemical Geology, 178, 197-210.

Sonney, R., Vuataz, F.-D., 2010. Use of Cl/Br Ratio to Decipher the Origin of Dissolved Mineral Components in Deep Fluids from the Alps Range and Neighbouring Areas. Proceedings World Geothermal Congress, Bali, Indonesia, 25-29 April 2010, 13pp.

Tackett, J.H., 2008. Lithologic controls of tiered pressure distribution in selected sedimentary basins. Master Thesis. USA, Oklahoma State University, 197pp.

Talukdar, S., Gallango, O., Ruggiero, A., 1988. Generation and migration of oil in the Maturin Sub-basin, Eastern Venezuelan Basin. Organic Geochemistry, 13(1-3), 537-547.

Talwani, M., 2002. The Orinoco Heavy Oil Belt in Venezuela (or Heavy oil to the rescue?), Energy Study: Latin America. The James A. Baker II Institute for Public Policy of Rice University. Houston, Texas, USA. 34pp. Accessible at: www.bakerinstitute.org/media/files/Research/8bb18b4e/the-orinoco-heavy-oil-belt-in-venezuela-or-heavy-oil-to-the-rescue.pdf [Last accessed: 12 June 2018]

Urbani, F., 1989. Geothermal reconnaissance of northeastern Venezuela. Geothermics, 18(3), 403-427.

Van Breukelen, M.R., Vonhof, H.B., Hellstrom, J.C., Wester, W.C.G., Kroon, D., 2008. Fossil dripwater in stalagmites reveals Holocene temperature and rainfall variation in Amazonia. Earth and Planetary Science Letters, 275(1-2), 54-60.

Warne, A.G., Guevara, E.H., Aslan, A., 2002. Late Quaternary Evolution of the Orinoco Delta, Venezuela. Journal of Coastal Research, 18, 225-253.

Manuscript received September 2017;
revision accepted April 2018;
published Online June 2018.

ELECTRONIC APPENDIX I

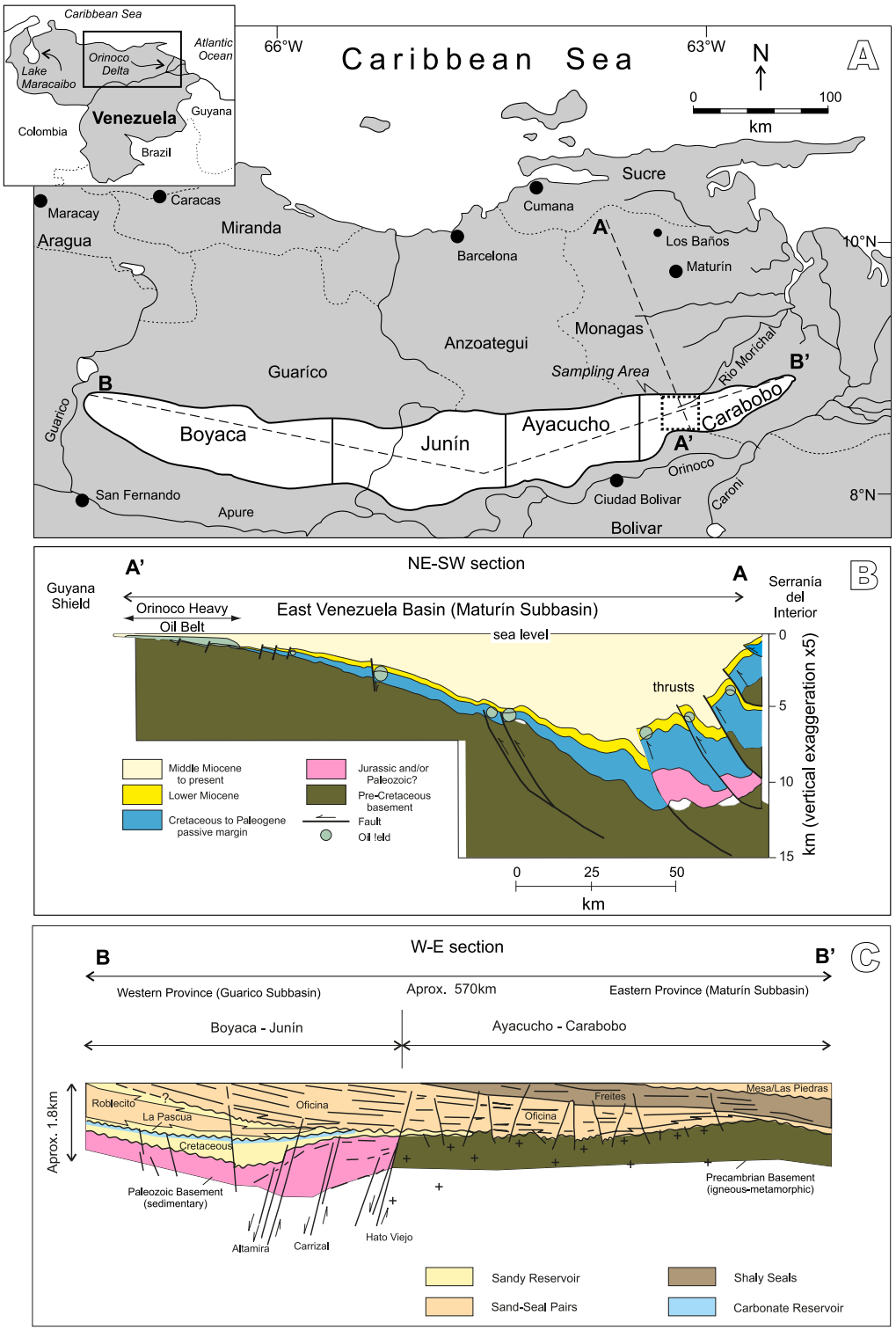

FIGURE I. A) Location map of the Faja Petrolífera del Orinoco "Hugo Chávez" (FPOHCh, in white) and sampling area in the Carabobo area, modified from Martinius *et al.* (2012) and Petroleos de Venezuela S.A.-Corporación Venezolana del Petróleo (2013). Continuous lines are rivers and creeks; thin dashed lines are the Venezuela states boundaries. B) NW-SE schematic cross section, modified from Schenk *et al.* (2009), see A) for location: A–A' dashed path. C) W-E cross section, modified from Audemard *et al.* (1985), see A) for location: B–B' dashed path.

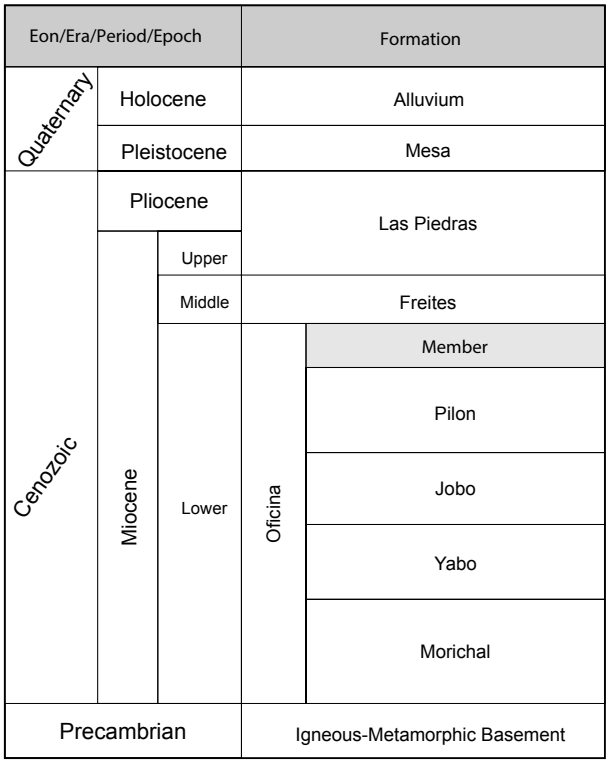

FIGURE II. Stratigraphic framework and age for the Carabobo area, modified from (Petróleos de Venezuela S.A., 1999).

TABLE I. Stratigraphic framework and age for the Carabobo area, modified from (Petróleos de Venezuela S.A., 1999)

*Well Code	Formation/Member	Depth m	Main Composition	pH	TDS (g/L)	Na^+ (mg/L)	K^+ (mg/L)	Ca^{2+} (mg/L)	Mg^{2+} (mg/L)	Cl^- (mg/L)	SO_4^{2-} (mg/L)	HCO_3^- (mg/L)	Li^+ (mg/L)	Sr^{2+} (mg/L)	B^{3+} (mg/L)	Si^{4+} (mg/L)	Br^- (mg/L)	$\delta^{18}O(H_2O)$ (‰ vs V-SMOW)	$\delta^2H(H_2O)$ (‰ vs V-SMOW)
C1-a	Freites	544	$Na\text{-}HCO_3$	-	1,0	186	79	40	2,0	81	15	550	-	-	-	12,2	-	-3,1	-34
C1-b	Freites	-	-	-	-	-	-	-	-	-	-	-	-	-	-	-	-	-3,3	-31
C2	Freites	-	-	-	-	59	2	-	-	103	7,8	1035	-	-	-	-	-	-	-
C3	Freites	429	Na-Cl	-	2,1	762	15	10	3,0	694	15	553	-	< 1	3,9	11,0	2,4	-	-
C4	Oficina/Morichal	-	Na-Cl	-	6,4	2324	108	28	77	3035	408	408	-	-	-	-	-	0,0	-5
C5	Oficina/Morichal	-	Na-Cl	7,3	8,5	2639	99	113	53	2727	< 5	2854	-	5,2	-	-	10,5	3,8	-5
C6	Oficina/Morichal	731	Na-Cl	-	9,3	2603	117	80	49	2738	9,5	3662	1,5	7,5	18	10,9	10,2	-	-
C7	Oficina/Morichal	733	Na-Cl	-	11,2	4227	142	181	79	5043	5,3	1500	2,7	12	24	10,6	19,6	-	-
C8	Oficina/Morichal	-	Na-Cl	8,3	11,4	3721	101	105	63	4085	89	3232	-	6,6	-	-	16,9	-2,0	-26
C9	Oficina/Morichal	-	Na-Cl	7,8	14,9	4609	116	174	133	6355	5,0	3516	-	7,7	-	-	26,9	-1,2	-7
C10	Oficina/Morichal	685	Na-Cl	-	15,3	4769	157	191	96	6160	11	3951	2,8	15	35	10,4	23,2	-	-
C11-a	Oficina/Morichal	-	Na-Cl	7,3	22,8	8126	233	86	166	10765	380	3048	-	33	-	-	63,5	-0,5	-6
C11-b	Oficina/Morichal	-	Na-Cl	-	27,6	8893	302	470	43	17200	41	674	-	-	24	-	63,5	1,0	-5
C12	Oficina/Morichal	-	Na-Cl	7,7	27,7	8402	216	332	156	15018	380	3171	-	40	-	-	66,8	-3,2	-23
C13	Oficina/Morichal	-	-	-	-	-	-	-	-	-	-	-	-	-	-	-	-	-4,8	-26
MP	Mesa/Las Piedras	-	-	-	<1	-	-	-	-	4,4	-	-	-	< 1	-	-	1,5	-2,3	-23
RM-a	Rio Morichal - Alluvium	-	-	6,6	<1	-	-	-	-	3,8	-	-	-	< 1	-	-	1,6	-1,6	-25
RM-b	Rio Morichal - Alluvium	-	-	-	-	-	-	-	-	-	-	-	-	-	-	-	-	-2,9	-27

*a: 2014-2015 sampling; b: 2016 sampling

-: not analyzed

TDS: calculated Total Dissolved Solids

< #: below detection limit

TABLE II. Preliminary chemical composition dataset of the Carabobo oilfield waters (2017 sampling campaign)

Code	pH	TDS	Na^+	K^+	Ca^{2+}	Mg^{2+}	Cl^-	SO_4^{2-}	HCO_3^-	Sr^{2+}	Br^-
		(g/L)	(mg/L)	(mg/L)	(mg/L)	(mg/L)	(mg/L)	(mg/L)	(mg/L)	(mg/L)	(mg/L)
P1	-	7	1725	99	64	38	1650	<5	3441	5	-
P2	7,14	8	1486	119	116	39	2182	<5	3276	5	13
P3	7,17	9	3076	189	205	29	4062	<5	1330	12	28
P4	6,86	10	2479	125	199	61	3469	<5	3306	8	22
P5	7,19	10	2934	188	283	18	5526	<5	1312	11	26
P6	7,08	10	3016	137	142	67	3662	<5	3380	7	20
P7	-	11	2846	120	16	44	3585	40	4160	3	-
P8	-	12	3819	203	116	40	6799	<5	1464	9	21
P9	7,22	15	4561	180	314	42	8365	<5	1238	16	34
P10	7,88	16	4742	203	12	101	7908	<5	3331	5	45
P11	7,15	17	4994	160	100	181	8181	<5	3416	12	46
P12	7,53	17	5449	210	97	115	8336	<5	3077	12	52
P13	7,69	18	5230	215	381	69	10900	<5	1220	23	59
P14	7,59	19	5935	228	431	99	10900	<5	1145	23	55
P15	-	20	6366	226	39	105	10500	<5	2494	10	50
P16	-	20	6364	250	72	110	10400	<5	2627	12	52
P17	7,15	21	6614	245	405	131	11800	<5	1770	16	74
P18	6,75	26	7327	251	415	194	15500	<5	1804	39	64
P19	6,83	31	7947	378	144	365	18600	<5	3001	28	89
P20	7,61	31	10200	326	50	102	16300	<5	3527	16	84
P21	-	31	14600	210	245	163	13700	<5	1703	16	-
P22	7,37	32	10132	291	123	181	16900	<5	4020	26	77
P23	-	32	7962	355	170	414	18700	<5	4014	39	87
P24	7,34	36	9685	297	519	554	20500	<5	3666	53	87
average	7,3	19	5812	217	194	136	9934	-	2655	17	52
median	7,2	18	5340	210	143	102	9383	-	3039	12	52
st.dev.	0,3	9	3160	74	147	133	5633	-	1039	13	25